NEURAL REGENERATION RESEARCH
December 2016, Volume 11, Issue 12
www.nrronline.org

RESEARCH ARTICLE

Electroacupuncture induces acute changes in cerebral cortical miRNA profile, improves cerebral blood flow and alleviates neurological deficits in a rat model of stroke

Hai-zhen Zheng[1, 2, #], Wei Jiang[3, #], Xiao-feng Zhao[1, *], Jing Du[2], Pan-gong Liu[2], Li-dan Chang[2], Wen-bo Li[2], Han-tong Hu[2], Xue-min Shi[1, 3]

1 VIP of Acupuncture Department, First Teaching Hospital of Tianjin University of Traditional Chinese Medicine, Tianjin, China
2 Tianjin University of Traditional Chinese Medicine, Tianjin, China
3 Department of Acupuncture and Moxibustion, First Teaching Hospital of Tianjin University of Traditional Chinese Medicine, Tianjin, China

How to cite this article: *Zheng HZ, Jiang W, Zhao XF, Du J, Liu PG, Chang LD, Li WB, Hu HT, Shi XM (2016) Electroacupuncture induces acute changes in cerebral cortical miRNA profile, improves cerebral blood flow and alleviates neurological deficits in a rat model of stroke. Neural Regen Res 11(12):1940-1950.*

Funding: *This work was supported by the National Natural Science Foundation of China, No. 81173416.*

Graphical Abstract

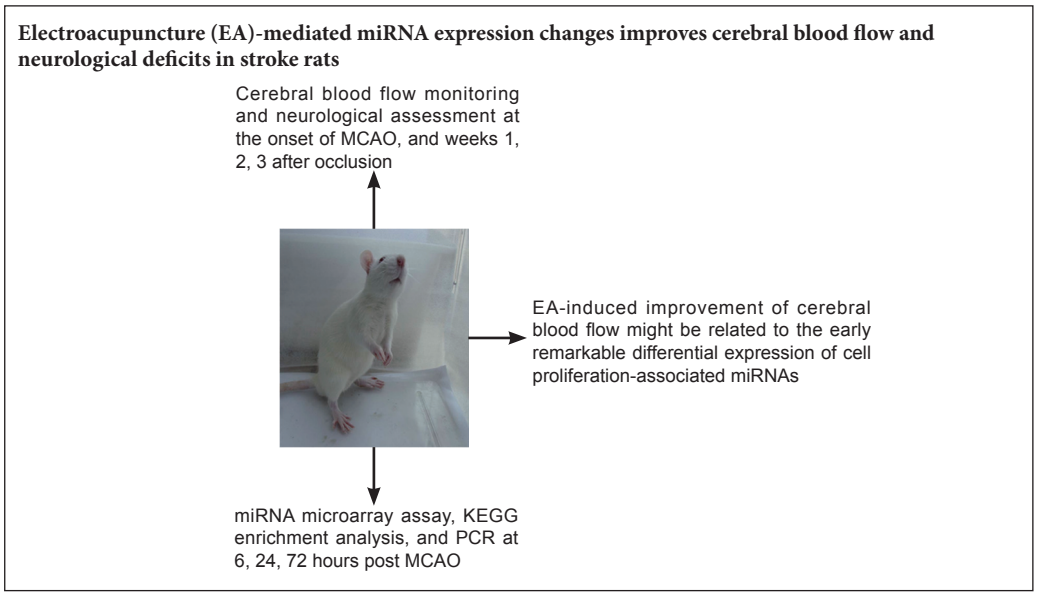

Correspondence to:
Xiao-feng Zhao,
zhxf67@163.com.

#These authors contributed equally to this study.

orcid:
0000-0002-1750-7364
(Xiao-feng Zhao)

doi: *10.4103/1673-5374.197135*

Accepted: *2016-11-16*

Abstract

Electroacupuncture has been shown to improve cerebral blood flow in animal models of stroke. However, it is unclear whether electroacupuncture alters miRNA expression in the cortex. In this study, we examined changes in the cerebral cortical miRNA profile, cerebral blood flow and neurological function induced by electroacupuncture in a rat model of stroke. Electroacupuncture was performed at *Renzhong* (GV26) and *Neiguan* (PC6), with a frequency of 2 Hz, continuous wave, current intensity of 3.0 mA, and stimulation time of 1 minute. Electroacupuncture increased cerebral blood flow and alleviated neurological impairment in the rats. miRNA microarray profiling revealed that the vascular endothelial growth factor signaling pathway, which links cell proliferation with stroke, was most significantly affected by electroacupuncture. Electroacupuncture induced changes in expression of rno-miR-206-3p, rno-miR-3473, rno-miR-6216 and rno-miR-494-3p, and these changes were confirmed by quantitative real-time polymerase chain reaction. Our findings suggest that changes in cell proliferation-associated miRNA expression induced by electroacupuncture might be associated with the improved cerebral blood supply and functional recovery following stroke.

Key Words: *nerve regeneration; stroke; middle cerebral artery occlusion; electroacupuncture; miRNA; cerebral blood flow; Neiguan (PC6); Renzhong (GV26); neural regeneration*

Introduction

Stroke is the third leading cause of death, and a leading cause of long-term disability (Selvamani et al., 2014). Ischemic stroke accounts for over 80% of the total number of strokes (Liu and Cheung, 2013). Focal cerebral ischemia elicits a specific and dynamic spatiotemporal pattern of gene expression (Küry et al., 2004; Rickhag et al., 2006). miRNAs, endogenous small, non-coding, single-stranded RNA molecules of ~22 nucleotides in length, are potent post-transcriptional regulators of gene expression (Hobert, 2008). miRNAs play pivotal roles in cell proliferation (Johnnidis et al., 2008), and therefore might contribute to the improvement in cerebral blood supply after stroke. Some studies have suggested that miRNAs may play an important role in the balance between neurological impairment and recovery in the acute phase of stroke (Hurtado et al., 2006).

Electroacupuncture (EA) is a combination of manual acupuncture and electrical stimulation. EA has been demonstrated to facilitate stroke recovery in patients and in the rat model of middle cerebral artery occlusion (MCAO) (Gao et al., 2006; Zhong et al., 2009; Kang et al., 2010; Kim et al., 2013). However, it is not known whether EA promotes functional recovery post ischemic stroke by regulating miRNA expression. *Renzhong* (GV26) and *Neiguan* (PC6) are the commonly used acupoints for stroke in China. *Renzhong* is located on the *Du* meridian, which is considered to be the sea of all the *yang* channels. *Neiguan*, is the *Luo* (connecting) point of the pericardium meridian. Needling both of these points can facilitate the resuscitation of the brain, thereby protecting against stroke events (Wang et al., 2011; Liu and Cheung, 2013).

Currently, there are no studies on the effects of EA on miRNA expression, and there is only limited data on its impact on cerebral blood flow. We hypothesized that EA may alter cell proliferation-associated miRNA expression in the acute phase, which might be associated with the cerebral blood flow increase and neurological functional recovery in the later stages.

In the present study, we evaluated cerebral blood flow and neurological function following stroke. In addition, we performed acute miRNA profiling in the cortex by miRNA microarray assay, finding the most significant pathways participating in the recovery process by enrichment analysis and the Kyoto Encyclopedia of Genes and Genomes (KEGG) database. Furthermore, the differential expression of cell proliferation-relevant miRNAs identified using the microarray chip was confirmed by quantitative real time-polymerase chain reaction (qRT-PCR) assay.

Materials and Methods

Ethics statement and experimental animals

The protocols for the care and use of animals complied with the National Institutes of Health Guide for the Care and Use of Laboratory Animals, and were approved by the Animal Ethics Committee of Tianjin University of Traditional Chinese Medicine of China (No. TCM-LAEC2012007). All possible efforts were made to minimize suffering and the number of rats used.

Twenty-five 8-week-old male Wistar rats, weighing 250–300 g, were purchased from the Laboratory Animal Center of PLA Academy of Military Medical Sciences (Beijing, China). The animals were housed at 23 ± 3°C and a relative humidity of 55 ± 5%, under a 12-hour light/dark cycle, and were provided with free access to food and water. Rats were randomly divided into normal control, MCAO, EA (MCAO + EA), and sham electroacupuncture (SA) (MCAO + SA) groups.

Rat MCAO model

The MCAO procedures were in accordance with Longa's method (Longa et al., 1989). Briefly, rats were intraperitoneally anesthetized with 10% chloral hydrate (300–330 mg/kg), and the left common carotid artery was exposed through an incision. The external and internal carotid arteries were carefully isolated. The common carotid artery was clamped, and the external carotid artery was suture-ligatured. Then, a nylon filament (diameter 0.26–0.285 mm) with a blunt tip was inserted into the lumen of the internal carotid artery to a distance of 16 to 18 mm. After the surgery, the rats were fed individually and kept warm. After regaining consciousness, they were allowed free access to water and food.

EA treatment

EA treatment was performed at *Renzhong* and *Neiguan* immediately after the MCAO rats fully recovered from anesthesia for 1 minute. The location of *Renzhong* is at the junction of the upper one-third and lower two-thirds of the cleft lip midline beneath the nasal septum. *Neiguan* is located between the tendons of palmaris longus and flexor carpi radialis at the flexor aspect of the forearm. SA stimulation was performed at two non-acupoints below the right costal region.

For the stimulation, 0.25 mm × 40 mm disposable filiform needles were used. When needling *Renzhong*, oblique puncturing toward the nasal septum to a depth of 2 mm was performed. For *Neiguan*, perpendicular puncturing to a depth of about 2 mm was done. EA and SA were delivered with a Han's acupoint nerve stimulator (HANS-200, Jisheng Medical Science and Technology Co., Ltd., Nanjing, Jiangsu Province, China). The parameters were as follows: frequency of 2 Hz, continuous wave, current intensity of 3.0 mA, and a stimulation duration of 1 minute. The Han's acupoint stimulator was connected to the inserted needles. EA and SA were performed immediately after full recovery from anesthesia. 24 hours' and 72 hours' groups of rats for RNA extraction were treated at an interval of 12 hours until 10 minutes before sacrifice. 6 hours' group of rats for RNA extraction were given the other treatment 10 minutes before sacrifice. Rats in the cerebral blood flow experiment received treatments at an interval of 12 hours until 1, 2 or 3 weeks post MCAO.

Cerebral blood flow velocity monitoring

A cohort of rats (n = 4 for the normal control, MCAO and EA groups; n = 5 for the SA group) were assigned for cerebral blood flow monitoring. Cerebral blood flow was measured using a laser-Doppler perfusion monitor (Moor, UK). Briefly, a small hole was drilled in the left parietal bone at a point 2 mm posterior to the bregma and 4 mm lateral to the sagittal suture, as previously described (Schäbitz et al., 2003). The laser Doppler probe (0.45 mm diameter) was inserted into the hole at a depth of 1 mm and fixed to the skull bone. The probe was used

to assess blood perfusion in the cortex by measuring cerebral blood flow velocity. Monitoring of cerebral blood flow velocity was performed at the onset of MCAO and at weeks 1, 2 and 3 following MCAO per group. As per the manufacturer's guidelines, the measured change in perfusion values was in the form of mL/min. All rats were killed after the final monitoring.

Neurological severity score (NSS)

Rats were evaluated for motor, sensory, reflex and balance dysfunctions with the NSS (Germanò et al., 1994). The NSS is a composite of motor, sensory, reflex and balance tests. In the severity rating scale, 1 point is given for the inability to perform the test or for the lack of a tested reflex; thus, the higher the score, the more severe the injury is. Rats with scores less than 7 or more than 12 after regaining consciousness from the MCAO operation were excluded. The tests were performed by two observers blinded to the groupings. All groups were evaluated at the onset of regaining consciousness from the MCAO operation, and at weeks 1, 2 and 3.

μParaflo™ miRNA microarray assay

The rats were killed at 6, 24 or 72 hours after MCAO (n = 2 for the normal control, MCAO, EA and SA groups). The cortex was rapidly isolated, frozen in liquid nitrogen, and stored at −80°C until extraction of total RNA. Microarray assay was performed using a service provider (LC Sciences, Houston, TX, USA). The assay used 2–5 μg of total RNA, which was size fractionated using a YM-100 Microcon centrifugal filter (Millipore, Sigma, CA, USA), and the small RNAs (< 300 nt) isolated were 3′-extended with a poly(A) tail using poly(A) polymerase. An oligonucleotide tag was then ligated to the poly(A) tail for later fluorescent dye staining; two different tags were used for the two RNA samples in dual-sample experiments. Hybridization was performed overnight on a μParaflo™ microfluidic chip using a micro-circulation pump (Atactic Technologies, Houston, TX, USA) (Gao et al., 2004; Zhu et al., 2007). On the microfluidic chip, each detection probe consisted of a chemically modified nucleotide coding a segment complementary to the target miRNA (miRBase Version 19, http://microrna.sanger.ac.uk/sequences/) or other RNA (control or customer defined sequences) and a spacer segment of polyethylene glycol to extend the coding segment away from the substrate. The detection probes were made by *in situ* synthesis using PGR (photogenerated reagent) chemistry. The hybridization melting temperatures were normalized by chemical modifications of the detection probes. Hybridization was performed using 100 μL 6× SSPE buffer (0.90 M NaCl, 60 mM Na_2HPO_4, 6 mM EDTA, pH 6.8) containing 25% formamide at 34°C. After hybridization, tag-specific Cy3 and Cy5 dyes were used for fluorescence labeling. Hybridization images were collected using a laser scanner (GenePix4000B, Molecular Devices, Sunnyvale, CA, USA) and digitized using Array-Pro image analysis software (Media Cybernetics, Rockville, MD, USA). Data were analyzed by first subtracting the background and then normalizing the signals using a LOWESS filter by locally-weighted regression (Bolstad et al., 2003). For two color experiments, the ratio of the two sets of detected signals was used (log_2-transformed, balanced).

Target prediction and enrichment analysis of signaling networks

We computationally predicted the targets of each altered miRNA using three different algorithms (PicTar, miRanda and TargetScan). The common predicted mRNAs were functionally annotated using the Kyoto Encyclopedia of Genes and Genomes database (Kanehisa and Goto, 2000). Next, 27 significantly differentially expressed miRNAs in the MCAO *vs*. normal cortex and the EA-treated *vs*. MCAO cortex at the various time points (log_2 value > 1.5 or < −1.5 for both intergroup comparisons at each time point) were subjected to enrichment analysis. The most significantly enriched KEGG pathways were subjected to miRNA-mRNA mapping.

MiRNA profile validation by qRT-PCR

Four miRNAs were selected after microarray analysis (the primers are listed in **Tables 1** and **2**). The reverse transcription reaction contained 250 ng total RNA, 0.5 μL 2 μM stem-loop RT primer, 1.0 μL 5× RT buffer, 0.6 μL RNase Free dH_2O and 0.4 μL PrimeScript RT Enzyme Mix I (TaKaRa Biotechnology (Dalian) Co., Ltd., Dalian, Liaoning Province, China). Reaction mixtures were incubated in an ABI PRISM 7900HT thermocycler (Applied Biosystems, Foster, CA, USA) for 15 minutes at 42°C, 5 seconds at 85°C, and held at 4°C. Reverse transcriptase reactions included no-template controls. A 0.5-μL aliquot of RT product (cDNA) was then mixed with 10.0 μL 2× SYBR Green Mix with ROX, 8.7 μL ddH_2O and 0.8 μL primer mix (10 μM) in a total volume of 20 μL for real-time PCR. Real-time PCR was performed using Platinum SYBR Green qPCR SuperMix-UDG (Invitrogen, Carlsbad, CA, USA). The reaction mixtures were incubated in a 96-well plate at 50°C for 2 minutes and 95°C for 2 minutes, followed by 39 cycles of 95°C for 15 seconds and 60°C for 30 seconds. All reactions were run in triplicate. U87 was used as the control miRNA. Ct values were normalized to U87, and fold changes were calculated using the $2^{-\Delta\Delta Ct}$ method. A higher normalized Ct value indicates a lower miRNA expression level.

Statistical analysis

SPSS 11.5 software (SPSS Inc., Chicago, IL, USA) was used for statistical analyses. Values were expressed as the mean ± SD. One sample Kolmogorov-Smirnov Test for nonparametric tests was performed to determine whether the values were normally distributed. Data were all normally distributed. Analysis of variance was used for among-group comparisons, followed by two-sample t-test for between-group comparison. Paired t-test was used for within-group comparison. Enrichment analysis was performed using Fisher's Exact Test. $P < 0.05$ was considered statistically significant.

Results

EA increased cerebral blood flow following MCAO

As shown in **Figure 1**, all the operated groups had a significant reduction (> 55%) (Traystman et al., 2001) in cerebral blood flow after MCAO. After EA treatment, cerebral blood flow increased consistently compared with the onset time point ($P < 0.05$) starting at week 1, up to week 3. The greatest cerebral blood supply was observed on week 3 in all the groups, with

Table 1 Primers for reverse transcription of miRNAs

Assay name	Sequence (5′–3′)	Primers for reverse transcriptase sequence (5′–3′)
rno-miR-206-3p	UGG AAU GUA AGG AAG UGU GUG G	CTC AGC GGC TGT CGT GGA CTG CGC GCT GCC GCT GAG CCA CAC AC
rno-miR-494-3p	TGA AAC ATA CAC GGG AAA CCT CT	GTC GTA TCC AGT GCA GGG TCC GAG GTA TTC GCA CTG GAT ACG ACA GAG GT
rno-miR-6216	GAT ACA CAG AGG CAG GAG GAG AA	GTC GTA TCC AGT GCA GGG TCC GAG GTA TTC GCA CTG GAT ACG ACT TCT CC
rno-miR-3473	TCT AGG GCT GGA GAG ATG GCT A	GTC GTA TCC AGT GCA GGG TCC GAG GTA TTC GCA CTG GAT ACG ACT AGC CA
rno-U87	ACA ATG ATG ACT TAT GTT TTT GCC GTT TAC CCA GCT GAG GGT TTC TTT GAA GAG AGA ATC TTA AGA CTG AGC	GCT CAG TCT TAA GAT TCT CT

rno-U87 was used as the internal reference miRNA.

Table 2 Primers for real-time polymerase chain reaction

Assay name	Forward primer (5′–3′)	Reversed primer (5′–3′)
rno-miR-206-3p	GGC GGT GGA ATG TAA GGA AG	GGC TGT CGT GGA CTG CG
rno-miR-494-3p	AGC CGC TTG AAA CAT ACA CG	CAG TGC AGG GTC CGA GGT
rno-miR-6216	GGT GGC GAT ACA CAG AGG C	CAG TGC AGG GTC CGA GGT
rno-miR-3473	CGG CGT TCT AGG GCT GG	CGC AGG GTC CGA GGT ATT C
rno-U87	ACA ATG ATG ACT TAT GTT TTT	GCT CAG TCT TAA GAT TCT CT

the EA group showing a significant increase compared with the MCAO group ($P < 0.05$). SA also improved cerebral blood flow, with a gradual increase from week 1 to week 2, and thereafter a slight reduction on week 3, relative to the onset time point ($P < 0.05$). Compared with the onset time point, MCAO rats also had elevated cerebral blood flow on weeks 1 and 2, although not statistically significant ($P > 0.05$).

EA alleviated neurological deficits in rats with MCAO

As shown in **Figure 2**, the NSS was substantially reduced in the MCAO, EA and SA groups. Compared with the MCAO group, EA reduced neurological deficits markedly from week 1 to week 2, while no significant difference was seen on week 3. The NSS was likewise significantly decreased compared with the SA group on weeks 2 and 3. There was no significant difference between the MCAO and SA groups.

MiRNA expression pattern in the cortex of rats with MCAO

In total, 503 mature miRNAs in release 19 of the Sanger miRBase database (http://microrna.sanger.ac.uk/sequences/) were expressed among all the groups, as evaluated with the microarray chip. 409, 416, 418 and 417 miRNAs were expressed in the cortex of normal controls, and the cortex of MCAO rats at 6, 24 and 72 hours, respectively.

Compared with the normal control, 114, 134 and 101 miRNAs were significantly differently expressed at 6, 24 and 72 hours, respectively, in the cortex of MCAO rats (transcripts with signals > 500; $P < 0.01$). Of these, 10, 32 and 9 miRNAs were markedly upregulated, while 11, 13 and 4 miRNAs were significantly downregulated at 6, 24 and 72 hours, respectively, in the MCAO cortex, compared with the normal control (fold change > 2 or < −2; **Table 3**). Other miRNAs with significant changes in expression of > 2 or < −2-fold, but low signals (< 500), were also identified (**Table 3**).

Seven miRNAs were identified with a cortical expression change of > 2-fold 6 hours post MCAO *vs.* control, 24 hours post MCAO *vs.* 6 hours post MCAO, and 72 hours post MCAO *vs.* 24 hours post MCAO. These were rno-miR-200b-3p, rno-miR-200a-3p, rno-miR-429, rno-miR-1306-3p, rno-miR-672-5p, rno-miR-328a-5p and rno-miR-377-3p. Among these, rno-miR-200b-3p and rno-miR-429 showed a significant upregulation 6 hours post MCAO. Thereafter, they returned to marginally elevated levels 24 hours post MCAO compared with control, and then again increased toward levels similar to 6 hours post MCAO. Some special miRNAs, with unique 7 to 9-bp signature motifs that target specific sets of gene promoters, were also detected in our samples, including rno-miR-347 (Gubern et al., 2013), rno-miR-331-3p, rno-miR-324-3p, rno-miR-324-5p, rno-miR-140-5p, rno-miR-145-5p, rno-miR-290 and rno-miR-214-3p (Dharap et al., 2009).

MiRNA expression profile after EA in the cortex of rats with MCAO

414, 395 and 405 miRNAs were detected in the cortex of MCAO rats given EA at 6, 24 and 72 hours, respectively. 124 miRNAs were expressed at significantly different levels between the EA and MCAO groups at 6 hours. Of these, 12 were upregulated and 3 were downregulated by > 2-fold (**Table 4**). 43 miRNAs were upregulated 1.1–2.0-fold, and 66 miRNAs were downregulated 1.1–2.0-fold. rno-miR-133b-5p showed the greatest fold change (84,708 *vs.* 7). At 24 hours, 145 miRNAs were expressed at significantly different levels in the EA group *vs.* the MCAO group. Of these, 35 and 17 miRNAs showed < −2-fold and > 2-fold changes in expression, respectively (**Table 4**). The fold changes among upregulated miRNAs ranged from 1.1 to 10.2, while the fold changes among downregulated miRNAs ranged from −1.2 to −7,896.4. The heat map of significantly differentially expressed miRNAs (Log_2 ratio > 1.5 or < −1.5) is shown in

Table 3 Fold change of significantly differentially expressed (> 2-fold or < −2-fold) miRNAs between middle cerebral artery occlusion and normal control groups

MiRNA	6 hours	24 hours	72 hours	*P*	MiRNA	6 hours	24 hours	72 hours	*P*
Altered at one time point					Altered at two time points				
rno-miR-568	2.9(0.000)	1.4(0.005)	−1.4(0.030)	0.000	rno-miR-290	**2.7**(0.001)	40.5(0.000)	1.8(0.006)	0.000
rno-miR-758-5p	1.9(0.000)	3.2(0.000)	1.0(0.477)	0.000	rno-miR-1306-3p	2.7(0.000)	6.8 (0.000)	1.0(0.965)	0.000
rno-miR-21-5p	1.8(0.000)	2.1(0.000)	1.1(0.065)	0.000	rno-miR-3588	13.6(0.000)	**5.1**(0.000)	−1.0(0.832)	0.000
rno-miR-1224	1.5(0.000)	12.5(0.000)	1.2(0.010)	0.000	rno-miR-3596a	3.7(0.000)	5.3(0.000)	−1.5(0.004)	0.000
rno-miR-324-3p	1.4(0.002)	2.2 (0.000)	1.0(0.977)	0.000	rno-miR-206-3p	3.4(0.000)	5.8(0.000)	−1.2(0.018)	0.000
rno-miR-3584-5p	1.2(0.005)	9.4(0.000)	1.1(0.028)	0.000	rno-miR-672-5p	2.5(0.000)	5.5(0.000)	−1.1(0.127)	0.000
rno-miR-652-5p	1.0(0.759)	11.6(0.000)	1.3(0.005)	0.000	rno-miR-200b-3p	79.9(0.000)	1.6(–)	76.5(0.000)	0.000
rno-miR-32-3p	1.8(0.000)	3.1(0.000)	−1.2 (0.014)	0.000	rno-miR-133b-5p	1.8(–)	16,321.8(0.000)	**10.1**(0.001)	0.000
rno-miR-483-5p	1.7(0.000)	3.8(0.000)	−1.1(0.076)	0.000	rno-miR-6216	1.4(0.004)	4.1(0.000)	2.9(0.003)	0.000
rno-miR-466d	1.5(0.002)	2.3(0.001)	−1.2(0.108)	0.000	rno-miR-665	**−2.1**(0.002)	15.6(0.000)	1.5(0.005)	0.000
rno-miR-6325	1.5(0.001)	4.1(0.000)	−1.2(0.018)	0.000	rno-miR-328a-5p	−2.4(0.000)	8.2(0.000)	1.4(0.008)	0.000
rno-miR-339-3p	1.3(0.001)	5.1(0.000)	−1.1(0.283)	0.000	rno-miR-92a-2-5p	**−8.8**(0.000)	5.7(0.000)	1.1(0.298)	0.000
rno-miR-466b-5p	1.3 (0.002)	4.8(0.000)	−1.1(0.060)	0.000	rno-miR-7a-1-3p	−2.2(0.001)	−3.5(0.000)	1.4(0.018)	0.000
rno-miR-214-3p	1.3(0.015)	3.1(0.000)	−1.2(0.065)	0.000	rno-miR-135b-5p	−2.3(0.003)	−2.6(0.000)	1.7(0.001)	0.000
rno-miR-19b-3p	1.8(0.001)	**−2.1**(0.000)	−1.0(0.371)	0.000	rno-miR-126a-5p	**−5.2**(0.000)	**−3.4**(0.000)	1.4(0.039)	0.000
rno-miR-101b-3p	1.4(0.000)	−2.2(0.000)	−1.0(0.390)	0.000	rno-miR-219-5p	−2.9 (0.001)	−2.5(0.003)	−1.4(0.019)	0.000
rno-miR-708-5p	1.1(0.071)	−2.3(0.000)	−1.0(0.386)	0.000	rno-miR-338-3p	−2.2(0.000)	−2.7(0.000)	−1.1(0.075)	0.000
rno-miR-301a-3p	1.0(0.675)	−3.8(0.000)	−1.3(0.004)	0.000	rno-miR-369-3p	−2.9(0.000)	−1.6(0.000)	2.6(0.001)	0.000
rno-miR-153-5p	1.0(0.981)	**−2.8**(0.000)	−1.2(0.030)	0.000	rno-miR-6215	−1.6 (0.000)	7.0(0.000)	2.2 (0.000)	0.000
rno-let-7e-5p	−2.4(0.000)	1.1(0.097)	−1.7(0.000)	0.000	Altered at three time points				
rno-miR-28-5p	**−2.8**(0.000)	−1.9(0.000)	−1.9(0.001)	0.000	rno-miR-429	372.7(0.005)	**4.8**(–)	359.7(0.005)	0.000
rno-miR-352	−2.7(0.000)	−1.0(0.857)	−1.6(0.000)	0.000	rno-miR-3556a	14.6(0.000)	**7.1**(0.000)	**2.3**(0.000)	0.000
rno-miR-129-2-3p	−2.1(0.000)	−1.3(0.000)	−1.1(0.030)	0.000	rno-miR-200a-3p	430.9(0.010)	**−4.7**(–)	434.9(0.010)	0.000
rno-miR-3594-5p	−1.0(0.693)	4.1(0.000)	1.0(0.883)	0.000	rno-miR-182	**3.3**(0.004)	**−2.7**(0.004)	9.1(0.001)	0.000
rno-miR-3473	−1.3(0.003)	21.5(0.000)	1.1(0.062)	0.000	rno-miR-208a-5p	**−2.7**(0.004)	31.9(0.000)	**4.9**(0.000)	0.000
rno-miR-494-3p	−1.5(0.000)	3.1(0.000)	1.6(0.000)	0.000	rno-miR-377-3p	−4.0(0.000)	−27.5(0.000)	**3.7**(0.019)	0.000
rno-miR-365-5p	−1.5(0.001)	11.0(0.000)	1.7(0.016)	0.000	rno-miR-135a-5p	−4.6(0.000)	−2.8(0.000)	3.0(0.002)	0.000
rno-miR-423-5p	−1.4(0.020)	3.0(0.000)	−1.2(0.001)	0.000					
rno-miR-99b-3p	−1.2(0.013)	4.3(0.000)	−1.0(0.878)	0.000					
rno-miR-210-3p	−1.2(0.070)	3.7(0.000)	−1.0(0.697)	0.000					
rno-let-7f-5p	−1.2(0.004)	1.3(0.002)	−2.1(0.000)	0.000					
rno-miR-551b-3p	−1.4(0.000)	−3.5(0.000)	−1.5(0.003)	0.000					
rno-miR-29b-3p	−1.7(0.001)	−2.5(0.000)	−1.1(0.114)	0.000					
rno-miR-451-5p	−1.8(0.000)	−2.9(0.000)	−1.3(0.000)	0.000					
rno-miR-181d-5p	−1.8(0.000)	−2.3(0.000)	1.1(0.090)	0.000					
rno-miR-664-1-5p	−1.1(0.195)	−1.0 (0.624)	2.2 (0.001)	0.000					

The number outside the brackets indicates the fold change *vs*. the normal control group. The numbers in the brackets indicate the *P* values of *t*-test for the fold change *vs*. the normal control group. The numbers in bold indicate the fold change of miRNAs which were not identified in the analysis of significantly differentially expressed miRNAs with signals > 500 at the corresponding time *vs*. the normal control. Analysis of variance was used for among-group comparison.

Figure 3. At 72 hours post stroke, compared with the MCAO group, EA elevated the expression of 3 miRNAs—rno-miR-133b-5p, rno-miR-411-3p and rno-miR-128-3p—by > 2-fold and downregulated 15 miRNAs by > 2-fold (**Table 4**).

MiRNA expression profile in the cortex of SA-treated rats with MCAO

422 miRNAs, 410 miRNAs and 413 miRNAs were detected in the cortex of SA-treated rats at 6, 24 and 72 hours after MCAO, respectively. 125 miRNAs were expressed at significantly different levels in the SA and MCAO groups at 6 hours. 16 and 5 miRNAs were expressed in a markedly upregulated and downregulated manner (fold change > 2 or < −2), respectively (**Table 5**). 56 miRNAs were downregulated 1.1–2.0-fold. 48 miRNAs were upregulated 1.2–2.0-fold. rno-miR-133b-5p was upregulated the greatest amount (31,777 *vs*. 7). rno-miR-133b-5p was barely expressed in the MCAO group, but was highly expressed in the SA group. At 24 hours, compared with the MCAO group, 88 miRNAs were significantly differentially expressed in the SA group. In the SA group, 2 miRNAs were changed < −2-fold, namely, rno-miR-290 (−2.1-fold) and rno-miR-133b-5p (−776.9-fold), and 5 miRNAs were increased > 2-fold, including rno-miR-377-3p (24.8-fold), rno-miR-135a-5p (3.8-fold), rno-miR-6216 (3.0-fold), rno-miR-135b-5p (2.8-fold) and rno-miR-181d-5p (2.4-fold). rno-miR-133b-5p was weakly detected in the SA group (85), but highly expressed in the MCAO group. rno-miR-377-3p was expressed in an opposite

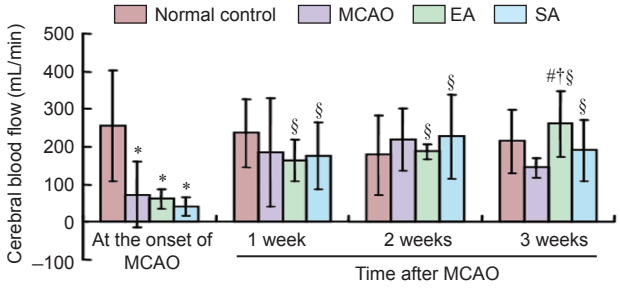

Figure 1 Cerebral blood flow among the various groups.
All data are presented as the mean ± SD. Analysis of variance was used for among-group comparison, followed by two-sample *t*-test for between-group comparison. Paired *t*-test was used for within-group comparison. **P* < 0.05, *vs.* normal control group; #*P* < 0.05, *vs.* MCAO group; †*P* < 0.05, *vs.* SA group; §*P* < 0.05, *vs.* the onset of MCAO. MCAO: Middle cerebral artery occlusion; EA: electroacupuncture; SA: sham electroacupuncture.

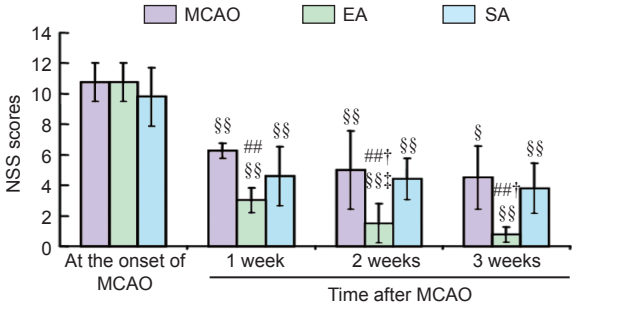

Figure 2 Effect of EA on neurological function in rats with MCAO.
Neurological function was assessed with the NSS. The higher the score, the more severe the injury is. All data are expressed as the mean ± SD. Analysis of variance was used for among-group comparison, followed by two independent samples *t*-test for between-group comparison. Paired *t*-test was used for within-group comparison. ##*P* < 0.01, *vs.* MCAO group; †*P* < 0.05, *vs.* SA group; §*P* < 0.05, §§*P* < 0.01, *vs.* the onset of MCAO; ‡*P* < 0.05, *vs.* 1 week after MCAO. MCAO: Middle cerebral artery occlusion; EA: electroacupuncture; SA: sham electroacupuncture; NSS: neurological severity score.

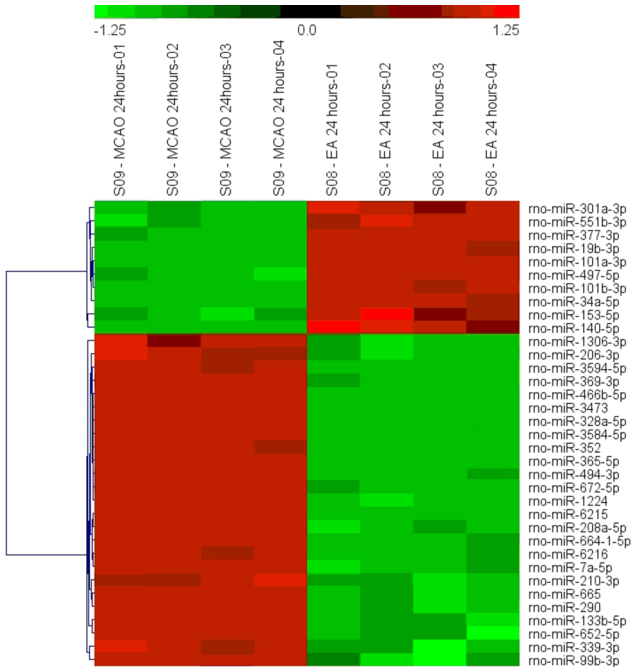

Figure 3 Heat map of significantly differentially expressed miRNAs (log ratio > 1.5 or < –1.5) in EA 24 hours *vs.* MCAO 24 hours.
Red indicates upregulation and green indicates downregulation in the EA group at 24 hours. MCAO: Middle cerebral artery occlusion; EA: electroacupuncture at *Renzhong* (GV26) and *Neiguan* (PC6).

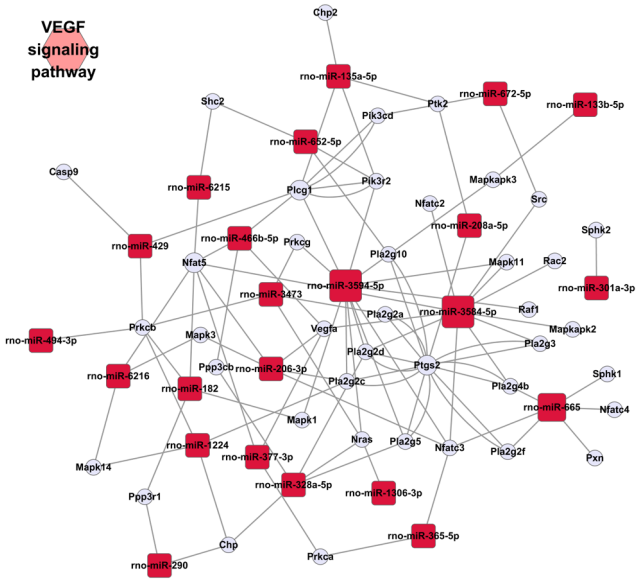

Figure 4 rno-miRNA-mRNA network affecting VEGF signaling pathway based on the first global prediction.
VEGF: Vascular endothelial growth factor.

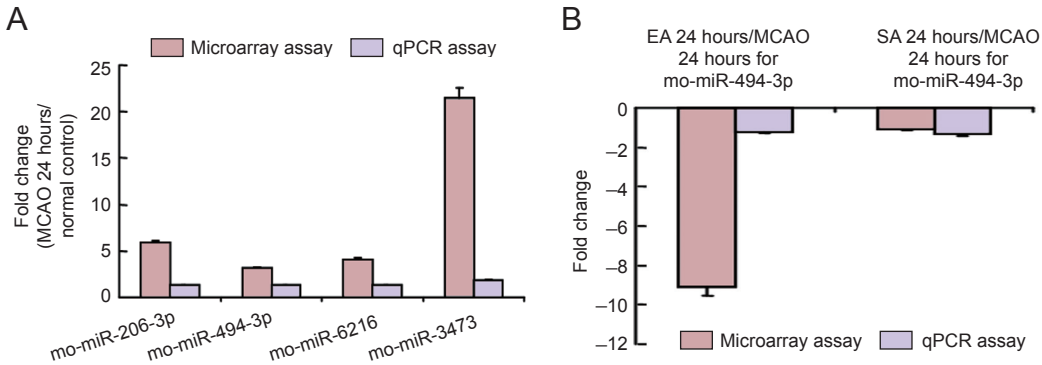

Figure 5 Validation of miRNA expression profiles by quantitative real time-PCR.

Validation of the expression profiles for rno-miR-206-3p, rno-miR-494-3p, rno-miR-6216 and rno-miR-3473 in the MCAO group at 24 hours *vs.* normal control (A), and rno-miR-494-3p in EA and SA groups *vs.* MCAO group at 24 hours (B), showing fold changes in microarray expression and quantitative real time-PCR using rno-U87 as a reference miRNA. Values are expressed as the mean ± SD. Statistical analysis was performed using unpaired *t*-test. MCAO: Middle cerebral artery occlusion; PCR: polymerase chain reaction; EA: electroacupuncture; SA: sham electroacupuncture.

Table 4 Fold change in cortical expression (> 2-fold or < –2-fold) between the EA and MCAO groups

MiRNA	*P* (*t* test)	Fold change	MiRNA	*P* (*t* test)	Fold change
At 6 hours			At 24 hours		
rno-miR-133b-5p	0.001	11,552.2	rno-miR-7a-5p	0.000	–2.9
rno-miR-758-5p	0.000	3.2	rno-miR-352	0.000	–3.1
rno-miR-210-5p	0.003	3.2	rno-miR-672-5p	0.000	–3.2
rno-miR-34c-3p	0.001	2.9	rno-miR-1306-3p	0.000	–3.4
rno-miR-196c-3p	0.000	2.6	rno-miR-206-3p	0.000	–3.4
rno-miR-423-5p	0.001	2.5	rno-miR-3594-5p	0.000	–3.8
rno-miR-568	0.000	2.4	rno-miR-339-3p	0.000	–3.9
rno-miR-466b-2-3p	0.000	2.4	rno-miR-369-3p	0.000	–4.2
rno-let-7e-5p	0.000	2.2	rno-miR-466b-5p	0.000	–4.3
rno-miR-466c-3p	0.000	2.2	rno-miR-99b-3p	0.001	–6.1
rno-miR-3596a	0.000	2.1	rno-miR-6216	0.000	–7.6
rno-miR-3574	0.002	2.1	rno-miR-664-1-5p	0.000	–8.0
rno-miR-21-5p	0.000	–2.1	rno-miR-3584-5p	0.000	–9.0
rno-miR-7a-1-3p	0.000	–2.2	rno-miR-494-3p	0.000	–9.1
rno-miR-377-3p	0.000	–8.7	rno-miR-1224	0.000	–10.9
At 24 hours			rno-miR-652-5p	0.000	–13.1
rno-miR-377-3p	0.000	10.2	rno-miR-6215	0.000	–14.4
rno-miR-19b-3p	0.000	6.0	rno-miR-328a-5p	0.000	–16.0
rno-miR-301a-3p	0.000	5.4	rno-miR-3473	0.000	–18.5
rno-miR-551b-3p	0.000	4.3	rno-miR-665	0.000	–21.2
rno-miR-34a-5p	0.000	4.3	rno-miR-290	0.000	–25.8
rno-miR-101b-3p	0.000	3.8	rno-miR-365-5p	0.000	–29.6
rno-miR-140-5p	0.000	3.7	rno-miR-208a-5p	0.000	–49.6
rno-miR-497-5p	0.000	3.2	rno-miR-133b-5p	0.000	–7,896.4
rno-miR-153-5p	0.000	3.1	At 72 hours		
rno-miR-101a-3p	0.000	3.1	rno-miR-133b-5p	0.000	893.7
rno-miR-138-5p	0.000	2.8	rno-miR-411-3p	0.000	2.3
rno-miR-106b-5p	0.000	2.8	rno-miR-128-3p	0.000	2.1
rno-miR-31a-5p	0.000	2.6	rno-miR-328a-5p	0.000	–2.1
rno-miR-708-5p	0.000	2.6	rno-miR-196c-3p	0.001	–2.1
rno-miR-29c-5p	0.000	2.5	rno-miR-181d-5p	0.003	–2.4
rno-miR-1843-5p	0.000	2.3	rno-miR-20b-5p	0.000	–2.5
rno-miR-154-5p	0.008	2.1	rno-miR-369-3p	0.000	–3.1
rno-miR-196c-3p	0.000	–2.1	rno-miR-7a-1-3p	0.000	–3.4
rno-miR-374-5p	0.000	–2.1	rno-miR-494-3p	0.000	–3.6
rno-miR-210-5p	0.000	–2.2	rno-miR-135b-5p	0.000	–3.7
rno-miR-6325	0.000	–2.2	rno-miR-28-5p	0.000	–4.1
rno-miR-335	0.000	–2.2	rno-miR-126a-5p	0.001	–4.4
rno-miR-384-3p	0.000	–2.3	rno-miR-664-1-5p	0.000	–9.5
rno-miR-466d	0.000	–2.4	rno-miR-135a-5p	0.000	–9.5
rno-miR-214-3p	0.000	–2.5	rno-miR-182	0.006	–13.0
rno-miR-423-5p	0.000	–2.7	rno-miR-377-3p	0.001	–47.7
rno-miR-483-5p	0.000	–2.8	rno-miR-429	0.005	–1,580.2
rno-miR-210-3p	0.000	–2.9			

MCAO: Middle cerebral artery occlusion; EA: electroacupuncture at *Renzhong* (GV26) and *Neiguan* (PC6).

manner (73 *vs*. 1,807 for MCAO *vs*. SA). 38 miRNAs were upregulated 1.1–2.0-fold, while 43 miRNAs were downregulated 1.2–2.0-fold. At 72 hours post MCAO, 178 miRNAs were significantly differentially expressed between the SA and MCAO groups. Among these, 64 and 48 miRNAs were increased and decreased, respectively, by > 2-fold (**Table 5**). 26 miRNAs were elevated 1.2–2.0-fold, while 40 miRNAs were reduced 1.1–2.0-fold.

MiRNA target prediction and functional analysis

In total, 2,062 mRNA targets were predicted for the detected miRNAs. Among the 27 dramatically changed miRNAs, no predicted targets were identified for rno-miR-377-3p, rno-miR-135a-5p and rno-miR-429. The enrichment analysis identified 28 KEGG pathways, with a *P* value < 0.05 by the Fisher's Exact Test. The top 10 KEGG pathways with *P* values < 0.05 are listed in **Table 6**. We also found that a miRNA may target a mRNA involved in multiple pathways, such as Mapk3, a putative target of rno-miR-6216, which participates in the top 10 pathways, including the vascular endothelial growth factor (VEGF) signaling pathway, long-term depression, toxoplasmosis, hepatitis C, gap junctions, GnRH signaling, glioma, melanogenesis, and the Fc epsilon RI signaling pathway, suggesting multiple functions of an miRNA in stroke etiology. Because the VEGF signaling pathway was the top significantly enriched pathway, we used Cytoscape

Table 5 Fold change (> 2-fold or < −2-fold) over MCAO at the indicated time point in the SA group

MiRNA	*P* (*t* test)	Fold change	MiRNA	*P* (*t* test)	Fold change	MiRNA	*P* (*t* test)	Fold change
At 6 hours			At 72 hours			At 72 hours		
rno-miR-133b-5p	0.001	4,333.7	rno-miR-3584-5p	0.000	5.4	rno-miR-219-5p	0.002	–2.2
rno-miR-183-5p	0.000	5.8	rno-miR-423-5p	0.000	5.4	rno-miR-425-5p	0.001	–2.2
rno-miR-34c-3p	0.000	4.5	rno-miR-1188-5p	0.001	4.8	rno-miR-186-5p	0.000	–2.3
rno-miR-210-5p	0.002	3.8	rno-miR-3574	0.000	4.6	rno-miR-410-3p	0.000	–2.3
rno-miR-758-5p	0.000	3.2	rno-miR-1224	0.000	4.4	rno-miR-494-3p	0.000	–2.4
rno-miR-568	0.000	3.0	rno-miR-21-5p	0.000	4.3	rno-miR-132-5p	0.000	–2.4
rno-miR-196c-3p	0.000	2.8	rno-miR-328a-5p	0.000	4.3	rno-miR-30a-5p	0.000	–2.4
rno-miR-466b-2-3p	0.000	2.7	rno-miR-483-5p	0.000	4.3	rno-miR-29c-3p	0.000	–2.5
rno-miR-423-5p	0.001	2.5	rno-miR-341	0.000	4.3	rno-miR-708-5p	0.000	–2.5
rno-miR-182	0.000	2.5	rno-miR-6215	0.000	3.8	rno-miR-369-5p	0.000	–2.5
rno-miR-3574	0.000	2.4	rno-miR-34c-3p	0.000	3.7	rno-miR-181d-5p	0.000	–2.6
rno-miR-466c-3p	0.000	2.4	rno-miR-466b-1-3p	0.000	3.6	rno-miR-338-3p	0.000	–2.6
rno-let-7d-3p	0.001	2.3	rno-miR-328a-3p	0.000	3.6	rno-miR-434-5p	0.001	–2.6
rno-miR-455-3p	0.000	2.3	rno-miR-324-3p	0.000	3.5	rno-miR-194-5p	0.000	–2.7
rno-miR-466b-1-3p	0.000	2.2	rno-miR-365-5p	0.000	3.4	rno-miR-30b-5p	0.000	–2.7
rno-miR-411-3p	0.000	2.1	rno-miR-485-3p	0.000	3.2	rno-miR-380-3p	0.001	–2.8
rno-miR-301a-3p	0.001	–2.1	rno-miR-455-3p	0.000	3.1	rno-miR-451-5p	0.000	–2.9
rno-miR-29b-3p	0.000	–2.2	rno-let-7c-5p	0.000	3.0	rno-miR-137-3p	0.000	–3.0
rno-miR-101a-3p	0.000	–2.3	rno-miR-667-3p	0.000	2.9	rno-miR-29a-5p	0.000	–3.1
rno-miR-19b-3p	0.000	–3.5	rno-miR-466c-3p	0.000	2.9	rno-miR-29b-3p	0.000	–3.1
rno-miR-377-3p	0.002	–4.0	rno-miR-92b-3p	0.000	2.8	rno-miR-582-5p	0.000	–3.1
At 72 hours			rno-let-7f-5p	0.000	2.8	rno-miR-409a-5p	0.001	–3.2
rno-miR-133b-5p	0.000	1,499.8	rno-miR-568	0.000	2.7	rno-miR-539-3p	0.000	–3.2
rno-miR-3593-3p	0.000	37.3	rno-let-7a-5p	0.000	2.7	rno-miR-411-5p	0.000	–3.2
rno-miR-1306-3p	0.000	14.6	rno-miR-346	0.000	2.7	rno-miR-30e-5p	0.000	–3.6
rno-miR-208a-5p	0.000	10.4	rno-miR-139-3p	0.000	2.6	rno-miR-28-5p	0.000	–3.6
rno-miR-667-5p	0.000	9.9	rno-miR-466b-2-3p	0.000	2.6	rno-miR-335	0.000	–3.6
rno-miR-339-3p	0.000	9.8	rno-let-7d-5p	0.000	2.5	rno-miR-499-5p	0.000	–3.6
rno-miR-3562	0.000	9.2	rno-miR-32-3p	0.001	2.5	rno-miR-337-3p	0.000	–3.6
rno-miR-195-3p	0.000	9.1	rno-miR-93-5p	0.000	2.5	rno-miR-664-1-5p	0.000	–3.6
rno-miR-672-5p	0.000	8.8	rno-miR-320-5p	0.000	2.5	rno-miR-340-5p	0.000	–4.2
rno-miR-702-5p	0.000	8.0	rno-let-7b-5p	0.000	2.5	rno-miR-384-3p	0.000	–4.2
rno-miR-6325	0.000	7.4	rno-miR-151-3p	0.003	2.5	rno-miR-136-3p	0.000	–4.6
rno-miR-210-3p	0.000	7.0	rno-miR-338-5p	0.000	2.4	rno-miR-153-3p	0.000	–4.8
rno-miR-206-3p	0.000	7.0	rno-miR-92a-3p	0.000	2.3	rno-miR-7a-1-3p	0.000	–5.0
rno-let-7d-3p	0.000	6.3	rno-miR-138-2-3p	0.002	2.3	rno-miR-376c-3p	0.001	–5.1
rno-miR-99b-3p	0.000	6.3	rno-miR-128-3p	0.000	2.2	rno-miR-376b-3p	0.000	–5.6
rno-miR-665	0.000	6.3	rno-miR-15b-5p	0.000	2.1	rno-miR-182	0.002	–8.1
rno-miR-3473	0.000	6.1	rno-miR-320-3p	0.000	2.1	rno-miR-200b-3p	0.000	–13.8
rno-miR-466b-5p	0.000	6.1	rno-miR-150-5p	0.000	2.1	rno-miR-369-3p	0.000	–14.8
rno-miR-652-5p	0.000	5.9	rno-miR-93-3p	0.000	2.1	rno-miR-135b-5p	0.000	–15.8
rno-miR-210-5p	0.000	5.9	rno-miR-495	0.000	–2.1	rno-miR-429	0.000	–19.7
rno-miR-758-5p	0.000	5.6	rno-miR-101a-3p	0.001	–2.1	rno-miR-200a-3p	0.000	–26.9
rno-miR-3594-5p	0.000	5.6	rno-miR-100-5p	0.000	–2.1	rno-miR-135a-5p	0.000	–38.6
rno-miR-214-3p	0.000	5.5	rno-miR-7a-5p	0.000	–2.2			

MCAO: Middle cerebral artery occlusion; SA: sham electroacupuncture at non-acupoints below the right costal region.

software for correlation mapping of the miRNAs and corresponding mRNAs in this pathway (**Figure 4**). 38 mRNAs were in the VEGF signaling pathway. Among the 560 significantly upregulated mRNAs, 24 mRNAs affected VEGF signaling pathway. rno-miR-6216, rno-miR-3594-5p, rno-miR-3584-5p, rno-miR-1224, rno-miR-672-5p, rno-miR-328a-5p, rno-miR-665, rno-miR-652-5p and rno-miR-3473 had direct targets in the VEGF signaling pathway.

Validation of microarray data by qRT-PCR

qRT-PCR was performed to confirm the microarray differential expression of rno-miR-494-3p, rno-miR-206-3p, rno-miR-6216 and rno-miR-3473 at 24 hours following MCAO *vs*. the normal (control) group, and rno-miR-494-3p at 24 hours in the EA group *vs*. the MCAO group at 24 hours. U87 was the endogenous control. The results were consistent with the microarray data (**Figure 5**).

Discussion

This study suggests that acute changes in cell proliferation-associated miRNA expression produced by EA might be related with improved cerebral blood supply and stroke recovery. Our study is the first to investigate the neuroprotective effect of EA and its impact on global miRNA profile

Table 6 Top 10 significantly enriched KEGG pathways and their rankings

KEGG pathway	Enrichment *P* value	Rank (%)
VEGF signaling pathway	0.000003	4.3
Long-term depression	0.000569	3.0
Toxoplasmosis	0.001114	5
Hepatitis C	0.001761	4.5
Gap junction	0.003085	2.9
GnRH signaling pathway	0.003611	3.8
Glioma	0.005293	2.5
Melanogenesis	0.006112	3.4
Fc epsilon RI signaling pathway	0.007427	3.0
Pancreatic secretion	0.0084	3.4

Significantly expressed miRNAs (*P* value < 0.01, $\log_2$ value > 1.5 or < −1.5) were selected for pathway analysis. Enrichment *P* value was used to indicate pathway significance. The ranks of the top 10 KEGG pathways with the most enrichment are presented as a percentage (total pathway number as 100%). Enrichment analysis was performed using Fisher's Exact Test. KEGG: Kyoto Encyclopedia of Genes and Genomes.

in a rat model of stroke. Our study was aimed at providing insight into the mechanisms involved in the pathogenesis of stroke as well as the processes that participate in the improvement of cerebral blood supply elicited by EA.

Correlation between neurological severity and EA-induced improvement of cerebral blood flow

Groups with moderate stroke will likely show the greatest responsiveness to EA (Shiflett, 2007; Kim et al., 2013). The neuroprotective effect of EA may be insufficient to positively impact cases of severe stroke, while cases of mild stroke may recover without intervention. Consequently, we chose a model of moderate injury to evaluate the efficacy of EA in treating MCAO. Our findings are consistent with those of previous studies (Shiflett, 2007; Kim et al., 2013). The neurological deficits were significantly alleviated in the EA groups, compared with the MCAO group, from week 1 to week 3. The efficacy of EA was dependent on acupoint specificity, as SA had no effect on neurological score in rats with MCAO.

An insufficient blood supply in the brain is the main cause of ischemic neuronal injury (Fahlenkmp et al., 2014; Weaver and Liu, 2015). Immediate cerebral blood perfusion is paramount for optimal neuronal recovery. Acupuncture has been reported to improve cerebral blood flow (Ratmansky et al., 2015; Yang et al., 2015). Angiotensin II receptors appear to play a key role in restoring the blood supply (Li et al., 2014), by promoting angiogenesis (Ratmansky et al., 2015; Yang et al., 2015), improving arterial pressure and resistance (Yang et al., 2015), suppressing ischemic cascades, and regulating cell proliferation-relevant miRNAs.

Stimulating PC6 significantly enhances gastric motility (Yang et al., 2013), helping to promote neurological functional recovery. Most rats will have suppressed gastric-intestinal motility, and in traditional Chinese medicine, the stomach is the original storage site of foods and drinks to supplement the blood, which transports necessary nutrients through the organic body, including the brain, thereby improving cerebral blood flow. Here, stimulating *Renzhong* and *Neiguan*, two primary acupoints of *Shi-shi* resuscitation acupuncture manipulation, increased cerebral blood supply, further supporting their importance in treating stroke.

miRNAs altered post MCAO

miRNAs, which are 20–25 nucleotides long, are emerging as important posttranscriptional regulators of gene expression in various species (Krol et al., 2010; Ebert and Sharp, 2012; Yates et al., 2013). From our profiling, we identified differentially expressed miRNAs among all the groups. Of these, rno-miR-328a-3p, rno-miR-99a-5p, rno-miR-181b-5p, rno-miR-181a-5p, rno-miR-539-5p, rno-miR-195-5p, rno-miR-181c-5p and rno-miR-379-5p, which were reported to have zero expression at 24 hours of focal cerebral ischemia (Jeyaseelan et al., 2008), were expressed at high levels.

Based on the predicted targets associated with neuronal function and our search results of the PubMed database, we selected rno-miR-206-3p, rno-miR-6216, rno-miR-3473 and rno-miR-494-3p at 24 hours post MCAO for qRT-PCR confirmation, among them rno-miR-494-3p has homologues in humans. Their validation by qRT-PCR prompted us to focus on these four miRNAs.

Cerebral ischemia can activate neuronal stem and precursor cells to migrate to the injured area. These cells contribute to angiogenesis, neurogenesis and synaptogenesis (Zhang et al., 2004). It was suggested that stroke sequelae might be worse in the absence of constitutive neurogenesis (Liu et al., 2014). As a miRNA can usually bind to several mRNAs, the miRNA can play various roles in stroke events. Here, we chose to highlight these miRNA-regulated cell proliferation mechanisms. The former ID of rno-miR-206-3p was rno-miR-206. rno-miR-206 is a muscle-specific miRNA that is a key regulator of muscle cell proliferation, differentiation, apoptosis, migration and angiogenesis (Dey et al., 2011; Zhang et al., 2011; Jalali et al., 2012; Li et al., 2012). Overexpression of rno-miR-206 was found to inhibit neural cell viability (Wang et al., 2012). Increased rno-miR-206 expression levels in cerebral ischemia might contribute to the progression of injury. In our study, rno-miR-206 was underexpressed at 72 hours post MCAO, resulting in neurogenesis, in part explaining the spontaneous recovery in our rat model beginning at week 1. rno-miR-494, the former ID of rno-miR-494-3p, has been found to target anti-apoptotic proteins. Overexpression of rno-miR-494 significantly decreases the levels of DJ-1 *in vitro* and renders cells more susceptible to oxidative stress, thereby contributing to oxidative stress-induced dopaminergic neuronal death (Xiong et al., 2014). Therefore, the marginal downregulation of rno-miR-494-3p at 6 hours and that of rno-miR-206 may help promote recovery.

Given the lack of published information on rno-miR-6216 and rno-miR-3473, we examined their putative targets to help clarify their function. Mapk3 is the predicted target of rno-miR-6216, and activation of the Mapk3 signaling pathway promotes neuronal precursor cell differentiation (Chan et al., 2013). Psen1 is the predicted target of rno-miR-3473. Presenilins, such as Psen1, are required for normal expression of the CREB target genes, including c-fos

and BDNF, which play key roles in neuronal survival (Saura et al., 2004). We found that both miRNAs were upregulated in the ischemic cortex at 24 hours (although downregulated subsequently), thereby likely aggravating neuronal injury. Accordingly, we hypothesize that these four validated miRNAs might influence common neurodegenerative and neuroprotective processes or pathways. Because enhanced cell proliferation promotes brain vascularization, these miRNAs may play critical roles in the improvement of cerebral blood flow after ischemic insult.

The impact of EA-induced changes in miRNA expression and the VEGF signaling pathway on brain repair after MCAO

EA induced substantial changes in miRNA expression following MCAO, consistent with published papers (Luo et al., 2014; Zhang et al., 2015). In our study, rno-miR-494 was elevated 24 hours post MCAO, but EA decreased its expression at 24 hours. Therefore, rno-miR-494 may mediate the neuroprotective effect of EA in cerebral ischemic injury.

miRNAs regulate various biological pathways. Enrichment analysis identified the VEGF signaling pathway as an important pathway in our present study, in contrast with other studies (Luo et al., 2014; Zhang et al., 2015). VEGF was found to stimulate adult neurogenesis and improve the morphology and migration of new neurons in the subventricular zone and dentate gyrus (Jin et al., 2002). VEGF induces adult neurogenesis following exposure to an enriched environment or voluntary exercise (Zhao et al., 2008), and it reduces apoptosis, suggesting that it may promote the survival of neuronal stem cells (Schänzer et al., 2004). In our study, neurogenesis and cell survival were likely key processes in recovery following the ischemic insult. SA treatment reduced rno-miR-494 levels minimally compared with EA treatment, underscoring the impact of EA on miRNA levels.

Our EA stimulation duration was only 1 minute, shorter than in previous studies (Liu and Cheung, 2013; Qin et al., 2013; Xu et al., 2013; Kim et al., 2014). The marked changes in miRNA profile suggest that a 1-minute stimulation period might be sufficient for efficacy. This is clinically important, as a short stimulation protocol can reduce patient anxiety and pain. The PubMed search identified no study with a short EA stimulation period comparable to ours (although a 1-minute stimulation period is occasionally used for manual acupuncture (Luo et al., 2014; Zhang et al., 2015)). The CNKI database search identified one article on quick stimulation at *Renzhong* and *Neiguan* (Yu and Shen, 2013), suggesting that short stimulation improves muscular tension better than a longer needling period. Because our present study is our first to use a short EA treatment period, further studies are needed to compare the efficacy of short and long stimulation periods.

The principle limitations of our study are the small sample size and the lack of a confirmed association between miRNA changes and cerebral blood flow. The present study is the first to investigate the effects of EA stimulation at *Renzhong* and *Neiguan* on miRNA changes in acute ischemic injury. We also assessed the long-term effect on cerebral blood flow and its role in improving neurological deficits. Our findings should help widen the application of resuscitation needling therapy in stroke treatment. Furthermore, our study highlights the importance of accurate acupoint location. Additional studies, with larger sample sizes, are required to clarify the link between EA, miRNA changes, protein expression, neurogenesis, angiogenesis, and cerebral blood supply.

Acknowledgments: *We would like to acknowledge staff members in LC Science of Houston, TX, USA and its Affiliated LC Science Biotechnology Corporation, Hangzhou, China, especially Jian-ning Liu and Jian-fang Zhu on biotechnological assistance.*

Author contributions: *XFZ conceived and designed the whole experiment. HZZ, WJ and PGL carried out MCAO experiment and electroacupuncture treatments. PGL monitored cerebral blood flow. WBL and HTH performed neurological deficits assessment. HTH, JD and LDC participated in bioinformatics database research. HZZ drafted the paper. PGL performed some statistical analysis. Academician XMS gave professional advices on drafting the paper. XFZ authorized the paper. All authors approved the final version of the paper.*

Conflicts of interest: *Figure 5 has been published in the form of conference abstract in Volume 6, Issue 6 of European Journal of Integrative Medicine in 2014.*

Plagiarism check: *This paper was screened twice using CrossCheck to verify originality before publication.*

Peer review: *This paper was double-blinded and stringently reviewed by international expert reviewers.*

References

Bolstad BM, Irizarry RA, Astrand M, Speed TP (2003) A comparison of normalization methods for high density oligonucleotide array data based on variance and bias. Bioinformatics 19:185-193.

Chan WS, Sideris A, Sutachan JJ, Montoya G JV, Blanck TJ, Recio-Pinto E (2013) Differential regulation of proliferation and neuronal differentiation in adult rat spinal cord neural stem/progenitors by ERK1/2, Akt, and PLCγ. Front Mol Neurosci 6:23.

Dey BK, Gagan J, Dutta A (2011) miR-206 and -486 induce myoblast differentiation by downregulating Pax7. Mol Cell Biol 31:203-214.

Dharap A, Bowen K, Place R, Li LC, Vemuganti R (2009) Transient focal ischemia induces extensive temporal changes in rat cerebral MicroRNAome. J Cereb Blood Flow Metab 29:675-687.

Ebert MS, Sharp PA (2012) Roles for microRNAs in conferring robustness to biological processes. Cell 149:515-524.

Fahlenkamp AV, Coburn M, de Prada A, Gereitzig N, Beyer C, Haase H, Rossaint R, Gempt J, Ryang YM (2014) Expression analysis following argon treatment in an in vivo model of transient middle cerebral artery occlusion in rats. Med Gas Res 4:11.

Gao H, Guo J, Zhao P, Cheng J (2006) Influences of electroacupuncture on the expression of insulin-like growth factor-1 following, focal cerebral ischemia in monkeys. Acupunct Electrother Res 31:259-272.

Gao X, Gulari E, Zhou X (2004) In situ synthesis of oligonucleotide microarrays. Biopolymers 73:579-596.

Germanò AF, Dixon CE, d'Avella D, Hayes RL, Tomasello F (1994) Behavioral deficits following experimental subarachnoid hemorrhage in the rat. J Neurotrauma 11:345-353.

Gubern C, Camós S, Ballesteros I, Rodríguez R, Romera VG, Cañadas R, Lizasoain I, Moro MA, Serena J, Mallolas J, Castellanos M (2013) miRNA expression is modulated over time after focal ischaemia: up-regulation of miR-347 promotes neuronal apoptosis. FEBS J 280:6233-6246.

Hobert O (2008) Gene regulation by transcription factors and microRNAs. Science 319:1785-1786.

Hurtado O, Pradillo JM, Alonso-Escolano D, Lorenzo P, Sobrino T, Castillo J, Lizasoain I, Moro MA (2006) Neurorepair vs Neuroprotection in Stroke. Cerebrovasc Dis 21 Suppl 2:54-63.

Jalali S, Ramanathan GK, Parthasarathy PT, Aljubran S, Galam L, Yunus A, Garcia S, Cox RR, Lockey RF, Kolliputi N (2012) Mir-206 regulates pulmonary artery smooth muscle cell proliferation and differentiation. PLoS One 7:e46808.

Jeyaseelan K, Lim KY, Armugam A (2008) MicroRNA expression in the blood and brain of rats subjected to transient focal ischemia by middle cerebral artery occlusion. Stroke 39:959-966.

Jin K, Zhu Y, Sun Y, Mao XO, Xie L, Greenberg DA (2002) Vascular endothelial growth factor (VEGF) stimulates neurogenesis in vitro and in vivo. Proc Natl Acad Sci U S A 99:11946-11950.

Johnnidis JB, Harris MH, Wheeler RT, Stehling-Sun S, Lam MH, Kirak O, Brummelkamp TR, Fleming MD, Camargo FD (2008) Regulation of progenitor cell proliferation and granulocyte function by microRNA-223. Nature 451:1125-1129.

Küry P, Schroeter M, Jander S (2004) Transcriptional response to circumscribed cortical brain ischemia: spatiotemporal patterns in ischemic vs. remote non-ischemic cortex. Eur J Neurosci 19:1708-1720.

Kanehisa M, Goto S (2000) KEGG: kyoto encyclopedia of genes and genomes. Nucleic Acids Res 28:27-30.

Kang KA, Shin ES, Hur J, Hasan MR, Lee H, Park HJ, Park HK, Kim YJ (2010) Acupuncture attenuates neuronal cell death in middle cerebral artery occlusion model of focal ischemia. Neurol Res 32 Suppl 1:84-87.

Kim JH, Choi KH, Jang YJ, Bae SS, Shin BC, Choi BT, Shin HK (2013) Electroacupuncture acutely improves cerebral blood flow and attenuates moderate ischemic injury via an endothelial mechanism in mice. PLoS One 8:e56736.

Kim YR, Kim HN, Ahn SM, Choi YH, Shin HK, Choi BT (2014) Electroacupuncture promotes post-stroke functional recovery via enhancing endogenous neurogenesis in mouse focal cerebral ischemia. PLoS One 9:e90000.

Krol J, Loedige I, Filipowicz W (2010) The widespread regulation of microRNA biogenesis, function and decay. Nat Rev Genet 11:597-610.

Li J, He J, Du Y, Cui J, Ma Y, Zhang X (2014) Electroacupuncture improves cerebral blood flow and attenuates moderate ischemic injury via Angiotensin II its receptors-mediated mechanism in rats. BMC Complement Altern Med 14:441.

Li L, Sarver AL, Alamgir S, Subramanian S (2012) Downregulation of microRNAs miR-1, -206 and -29 stabilizes PAX3 and CCND2 expression in rhabdomyosarcoma. Lab Invest 92:571-583.

Liu L, Cheung RTF (2013) Effects of pretreatment with a combination of melatonin and electroacupuncture in a rat model of transient focal cerebral ischemia. Evid Based Complement Alternat Med 2013:953162.

Liu X, Ye R, Yan T, Yu SP, Wei L, Xu G, Fan X, Jiang Y, Stetler RA, Liu G, Chen J (2014) Cell based therapies for ischemic stroke: From basic science to bedside. Prog Neurobiol 115:92-115.

Longa EZ, Weinstein PR, Carlson S, Cummins R (1989) Reversible middle cerebral artery occlusion without craniectomy in rats. Stroke 20:84-91.

Luo D, Fan X, Ma C, Fan T, Wang X, Chang N, Li L, Zhang Y, Meng Z, Wang S, Shi X (2014) A Study on the Effect of neurogenesis and regulation of GSK3β/PP2A expression in acupuncture treatment of neural functional damage caused by focal ischemia in mcao rats. Evid Based Complement Alternat Med 2014:962343.

Qin WY, Luo Y, Chen L, Tao T, Li Y, Cai YL, Li YH (2013) Electroacupuncture could regulate the NF-κB signaling pathway to ameliorate the inflammatory injury in focal cerebral ischemia/reperfusion model rats. Evid Based Complement Alternat Med 2013:924541.

Ratmansky M, Levy A, Messinger A, Birg A, Front L, Treger I (2015) The effects of acupuncture on cerebral blood flow in post-stroke patients: a randomized controlled trial. J Altern Complement Med 22:33-37.

Rickhag M, Wieloch T, Gidö G, Elmér E, Krogh M, Murray J, Lohr S, Bitter H, Chin DJ, Von Schack D, Shamloo M, Nikolich K (2006) Comprehensive regional and temporal gene expression profiling of the rat brain during the first 24 h after experimental stroke identifies dynamic ischemia-induced gene expression patterns, and reveals a biphasic activation of genes in surviving tissue. J Neurochem 96:14-29.

Saura CA, Choi SY, Beglopoulos V, Malkani S, Zhang D, Rao BSS, Chattarji S, Kelleher RJ 3rd, Kandel ER, Duff K, Kirkwood A, Shen J (2004) Loss of presenilin function causes impairments of memory and synaptic plasticity followed by age-dependent neurodegeneration. Neuron 42:23-36.

Schäbitz WR, Kollmar R, Schwaninger M, Juettler E, Bardutzky J, Schölzke MN, Sommer C, Schwab S (2003) Neuroprotective effect of granulocyte colony-stimulating factor after focal cerebral ischemia. Stroke 34:745-751.

Schänzer A, Wachs FP, Wilhelm D, Acker T, Cooper-Kuhn C, Beck H, Winkler J, Aigner L, Plate KH, Kuhn HG (2004) Direct stimulation of adult neural stem cells in vitro and neurogenesis in vivo by vascular endothelial growth factor. Brain Pathol 14:237-248.

Selvamani A, Williams MH, Miranda RC, Sohrabji F (2014) Circulating miRNA profiles provide a biomarker for severity of stroke outcomes associated with age and sex in a rat model. Clin Sci (Lond) 127:77-89.

Shiflett SC (2007) Does acupuncture work for stroke rehabilitation: what do recent clinical trials really show? Top Stroke Rehabil 14:40-58.

Traystman RJ, Klaus JA, DeVries AC, Shaivitz AB, Hurn PD (2001) Anticonvulsant lamotrigine administered on reperfusion fails to improve experimental stroke outcomes. Stroke 32:783-787.

Wang Q, Li X, Chen Y, Wang F, Yang Q, Chen S, Min Y, Li X, Xiong L (2011) Activation of epsilon protein kinase C-mediated anti-apoptosis is involved in rapid tolerance induced by electroacupuncture pretreatment through cannabinoid receptor type 1. Stroke 42:389-396.

Wang R, Hu Y, Song G, Hao CJ, Cui Y, Xia HF, Ma X (2012) MiR-206 regulates neural cells proliferation and apoptosis via Otx2. Cell Physiol Biochem 29:381-390.

Weaver J, Liu KJ (2015) Does normobaric hyperoxia increase oxidative stress in acute ischemic stroke? A critical review of the literature. Med Gas Res 5:11.

Xiong R, Wang Z, Zhao Z, Li H, Chen W, Zhang B, Wang L, Wu L, Li W, Ding J, Chen S (2014) MicroRNA-494 reduces DJ-1 expression and exacerbates neurodegeneration. Neurobiol Aging 35:705-714.

Xu MS, Zhang SJ, Zhao D, Liu CY, Li CZ, Chen CY, Li LH, Li MZ, Xu J, Ge LB (2013) Electroacupuncture-Induced Neuroprotection against Cerebral Ischemia in Rats: Role of the Dopamine D2 Receptor. Evid Based Complement Alternat Med 2013:137631.

Yang L, Sui J, Shi H (2015) Control modeling and Chinese acupuncture treatment on cerebral circulation. Technol Health Care 23 Suppl 1:S77-82.

Yang ZK, Wu ML, Xin JJ, He W, Su YS, Shi H, Wang XY, Hu L, Jing XH, Litscher G (2013) Manual acupuncture and laser acupuncture for autonomic regulations in rats: observation on heart rate variability and gastric motility. Evid Based Complement Alternat Med 2013:276320.

Yates Luke A, Norbury Chris J, Gilbert Robert J (2013) The long and short of microRNA. Cell 153:516-519.

Yu C, Shen B (2013) Effect of quick acupuncture stimulation without retention on the neurologiacal deficits of ischemic stroke patients. Zhongguo Zhongyiyao Xinxi Zazhi 20:78-79.

Zhang C, Wen Y, Fan X, Yang S, Tian G, Zhou X, Chen Y, Meng Z (2015) A microarray study of middle cerebral occlusion rat brain with acupuncture intervention. Evid Based Complement Alternat Med 2015:496932.

Zhang R, Zhang Z, Wang L, Wang Y, Gousev A, Zhang L, Ho KL, Morshead C, Chopp M (2004) Activated neural stem cells contribute to stroke-induced neurogenesis and neuroblast migration toward the infarct boundary in adult rats. J Cereb Blood Flow Metab 24:441-448.

Zhang T, Liu M, Wang C, Lin C, Sun Y, Jin D (2011) Down-regulation of MiR-206 promotes proliferation and invasion of laryngeal cancer by regulating VEGF expression. Anticancer Res 31:3859-3863.

Zhao C, Deng W, Gage FH (2008) Mechanisms and functional implications of adult neurogenesis. Cell 132:645-660.

Zhong S, Li Z, Huan L, Chen BY (2009) Neurochemical Mechanism of Electroacupuncture: Anti-injury Effect on Cerebral Function after Focal Cerebral Ischemia in Rats. Evid Based Complement Alternat Med 6:51-56.

Zhu Q, Hong A, Sheng N, Zhang X, Matejko A, Jun KY, Srivannavit O, Gulari E, Gao X, Zhou X (2007) microParaflo biochip for nucleic acid and protein analysis. Methods Mol Biol 382:287-312.

Copyedited by Patel B, Yajima W, Yu J, Qiu Y, Li CH, Song LP, Zhao M